

Smoothed Particle Hydrodynamics Simulations for Asteroid Deflection

Maximilian Rutz

Abstract

Fragen:

- Wie viele gedruckte Exemplare? - Abstract und Introduction?

Contents

1	Introduction	3
2	Theory	4
2.1	Smoothed Particle Hydrodynamics	4
2.2	Miluphcuda SPH code	5
2.2.1	Equation of State	5
2.2.2	Porosity model	5
2.2.3	Strength model	6
2.2.4	Time Integration	6
3	Numerical Setup	7
3.1	Initial conditions	7
3.2	Material parameters	8
4	Results	10
4.1	Cratering	10
4.2	Beta factor	10
5	Discussion	14

1 Introduction

Bolide events 1994-2013
(Small asteroids that disintegrated in the Earth's atmosphere)

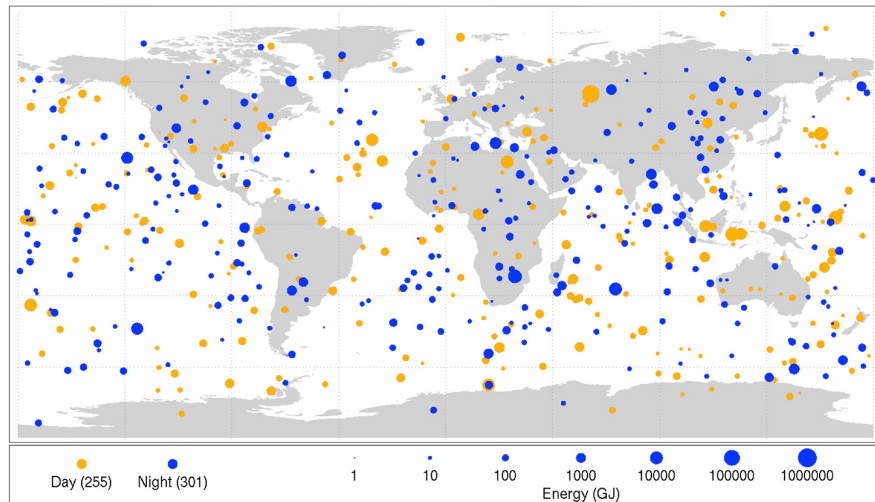


Figure 1: Past impacts [7]

- test case for p-alpha porosity and pressure dependent yield strength
 - Raducan [6] grid based 2d sims - Stickle [5]

2 Theory

2.1 Smoothed Particle Hydrodynamics

Smoothed Particle Hydrodynamics is a numerical simulation method first introduced by [2] in 1977. It is a Lagrangian particle method and as such often used when the geometry of the underlying problem makes it difficult to apply Eulerian grid-based methods like finite difference schemes. Although SPH is most often used to model liquids, it is possible to add physical models for solids as well.

A SPH simulation is composed of many individual SPH particles. Each particle moves through space with a velocity \vec{v} and a mass m . In contrast to particle methods used for N-body simulations or molecular dynamics, SPH particles carry information about continuous variables such as the density ρ or energy e . The particles only act as computational points at which equations from hydrodynamics/continuum mechanics such as the Euler or Navier-Stokes Equations are evaluated. Solving such equations comes down to converting partial differential equations to a system of first order ordinary differential equations in time.

$$\frac{d\vec{y}}{dt} = f(t, \vec{y}(t), A_1, \dots, A_n) \quad (1)$$

In equation 1 \vec{y} is a vector of quantities to be projected forward in time and A_1 through A_n are quantities that are calculated at every step. Once A_1 through A_n are known for every particle and the right hand side of quation 1 can be evaluated, standard integrators such as Runge-Kutta or Predictor-Corrector methods are used to update \vec{y} .

To calculate a quantity A at a particle location, SPH uses a weighted average of A over all particles in the neighborhood:

$$A(\vec{r}) \approx \int A(\vec{r}') W(\vec{r} - \vec{r}', h) d\vec{r}' \quad (2)$$

The kernel function $W(|\vec{r} - \vec{r}'|, h)$ at the particle location \vec{r} depends upon the distance to the other particles and a specific length h called the smoothing length. Most kernels used today have compact support within a radius of h . To ensure normalization of the kernel

$$\int W(\vec{r} - \vec{r}', h) d\vec{r}' = 1 \quad (3)$$

in the practical case of a finite number of particles, the density is added to

$$A_S(\vec{r}) = \lim_{h \rightarrow \infty} \int \frac{A(\vec{r}')}{\rho(\vec{r}')} W(\vec{r} - \vec{r}', h) \rho(\vec{r}') d\vec{r}' \propto \sum_{b=1}^N m_b \frac{A_b}{\rho_b} W(\vec{r} - \vec{r}', h) = A_b \quad (4)$$

$$\int W(|\vec{r} - \vec{r}'|, h) dr' = 0 \quad (5)$$

Figure 2 illustrates

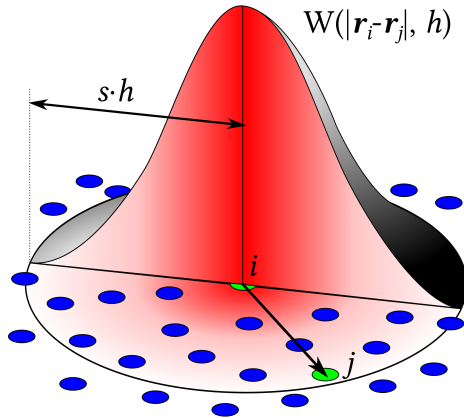


Figure 2: Kernel function [8]

2.2 Miluphcuda SPH code

Miluphcuda is a GPU accelerated smoothed particle hydrodynamics code that has been developed over several years at the University of Tuebingen by Christoph Schaefer and others. Its general use is well documented in [4]. Since the publication of the paper additional models for porosity and strength have been implemented.

2.2.1 Equation of State

The Tillotson equation of state [1]

2.2.2 Porosity model

There are different ways in which porosity can be modeled depending on the pore size. Depending on the simulation, macro porosity with pore sizes above the resolution of the simulation can be accounted for in the initial conditions. This however becomes impossible for granular material with sub-resolution sized grains and pores.

Microporosity models porosity as an additional material property and can be applied independently of the resolution.

In these simulations, a microporosity p- α model as outlined in [3] is used. The distention $\alpha \in [1, \infty)$ relates the current density ρ to the solid density ρ_s which is reached if the material is fully compressed. For a non-porous material α equals one.

$$\alpha \equiv \frac{\rho_s}{\rho} \quad (6)$$

Often the porosity ϕ is used instead of the distention α . They relate by

$$\phi = 1 - \frac{1}{\alpha} \quad (7)$$

Quadratic crush curve

2.2.3 Strength model

2.2.4 Time Integration

3 Numerical Setup

3.1 Initial conditions

- resolution bound to variable smoothing length - SPH needs uniform macro structure but random micro structure

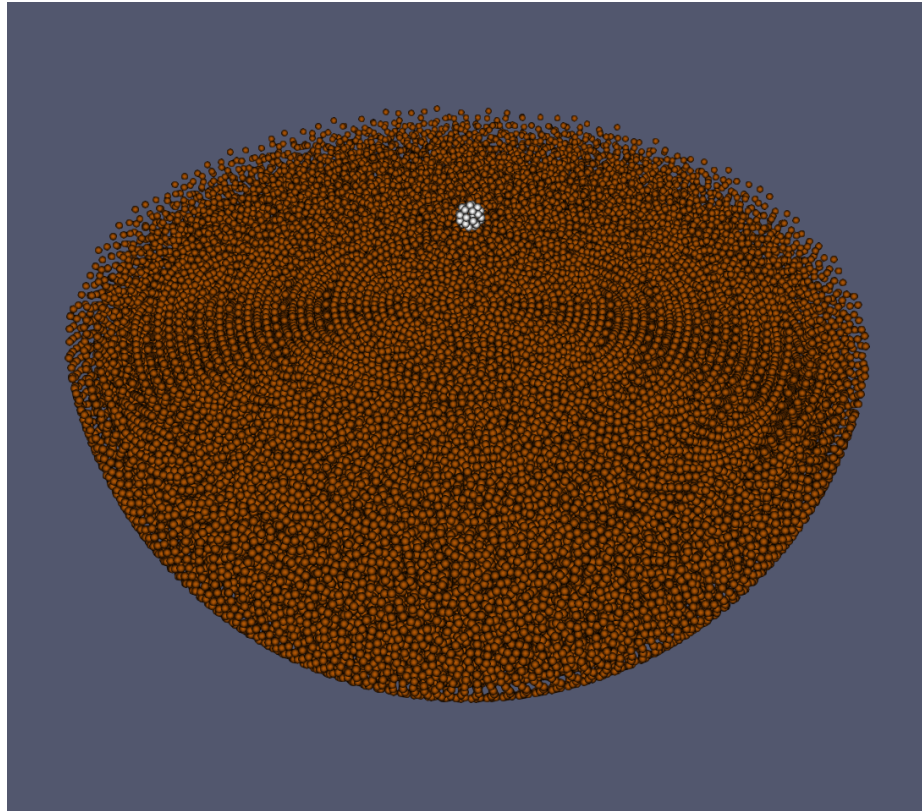


Figure 3: initial conditions

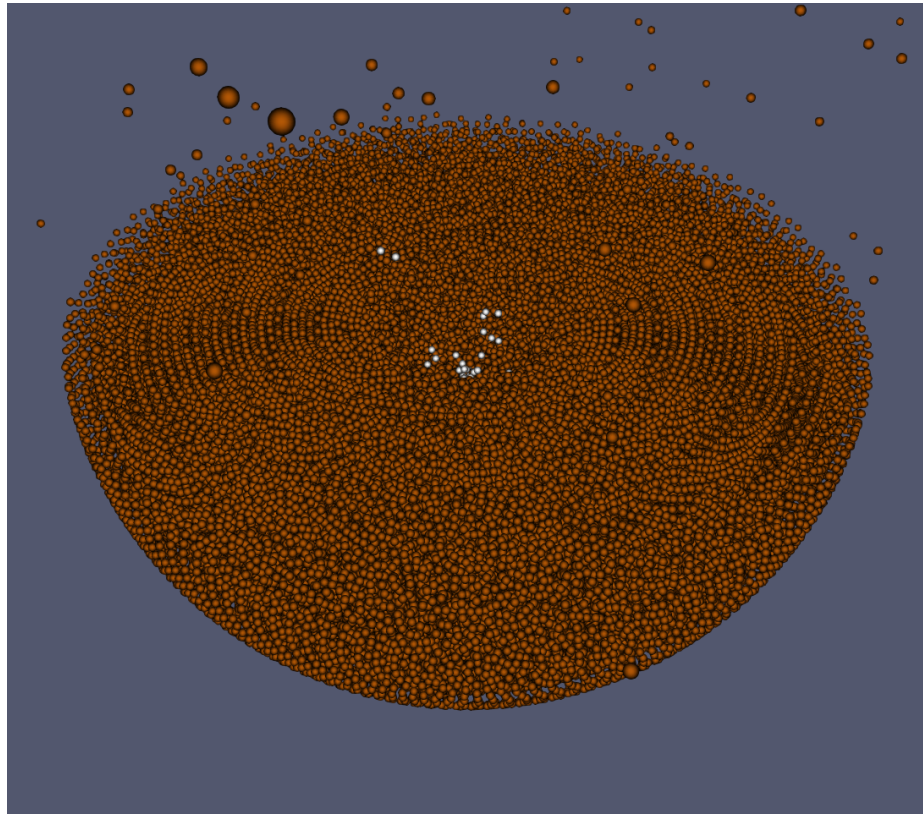


Figure 4: cratering of half sphere

3.2 Material parameters

- variable smoothing length min 0.1 bis max 10.0 - rholimit 0.95

Basalt target parameters			
Tillotson EOS	ρ_0	$2.86 \cdot 10^3 g \cdot cm^{-3}$	$2.70 \cdot 10^3 g \cdot cm^{-3}$
	A_T	$2.67 \cdot 10^{10} Pa$	$7.52 \cdot 10^{10} Pa$
	B_T	$2.67 \cdot 10^{10} Pa$	$6.50 \cdot 10^{10} Pa$
	E_0	$4.87 \cdot 10^8 J$	$5.00 \cdot 10^6 J$
	E_{iv}	$4.72 \cdot 10^6 J$	$3.00 \cdot 10^6 J$
	E_{cv}	$1.82 \cdot 10^7 J$	$1.39 \cdot 10^7 J$
	a_T	0.5	0.5
	b_T	1.5	1.63
	α_T	5.0	5.0
	β_T	5.0	5.0
Porosity	α_0	varying	not porous
	$p_{elastic}$	$1.0 \cdot 10^6 Pa$	not porous
	$p_{transition}$	$6.8 \cdot 10^7 Pa$	not porous
	$p_{compacted}$	$2.13 \cdot 10^8 Pa$	not porous
	α_e	4.64	not porous
	α_t	1.90	not porous
	c_s	$100.0 m \cdot s^{-1}$	not porous
Strength	cohesive strength Y_c	varying	$1.0 \cdot 10^9 Pa$
	α	0.982793 rad	0 rad
	$\alpha_{damaged}$	0.540419 rad	0 rad
	shear modulus μ	$2.27 \cdot 10^{10} Pa$	$2.69 \cdot 10^{10} Pa$
	bulk modulus K_0	$2.67 \cdot 10^{10} Pa$	$5.23 \cdot 10^{10} Pa$
	yield stress Y_0	$3.5 \cdot 10^9 Pa$	$2.76 \cdot 10^8 Pa$
Weibull	M	16	no damage
	K	$1.0 \cdot 10^{61}$	no damage
Artificial viscosity	α	1.0	1.0
	β	2.0	2.0

Table 1: Target parameters

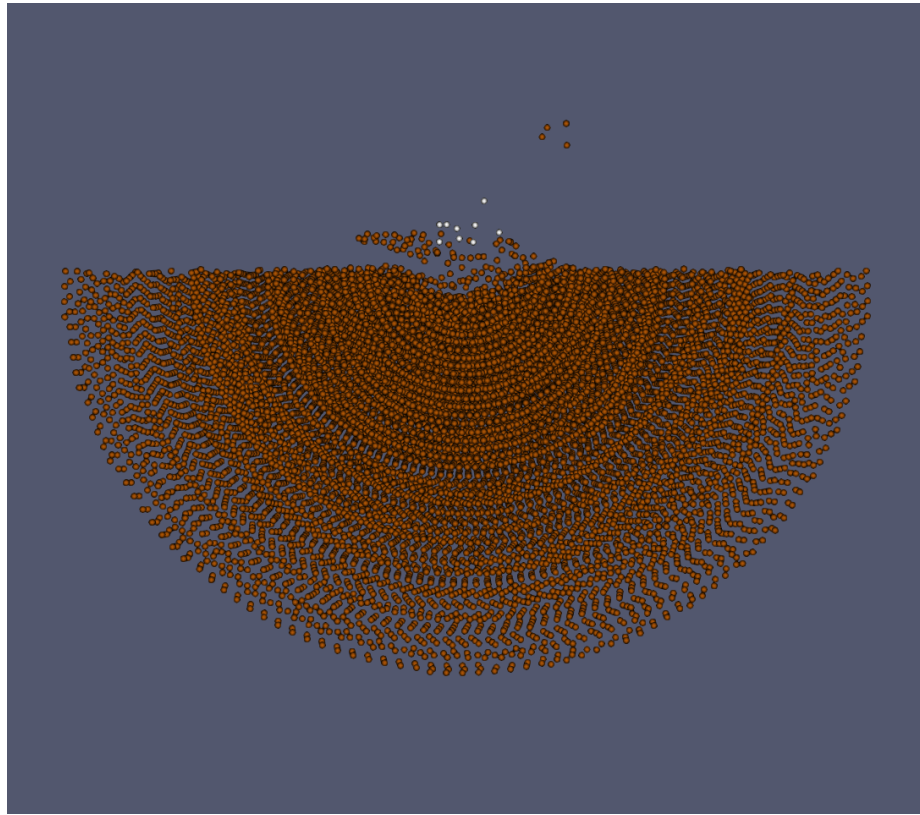


Figure 5: No porosity (0%), high strength ($Y=1\text{MPa}$)

4 Results

The simulations were run with porosities of 0%, 17%, 33% and 50% and cohesive strengths of 1kPa, 10kPa, 100kPa and 1MPa under impact angles of 0 and 45 degrees. This yields 32 simulations in total.

4.1 Cratering

Figures 5 through 8 show the effects of porosity and strength on the crater formation. The higher the porosity and the lower the porosity become, the wider and deeper the crater gets.

4.2 Beta factor

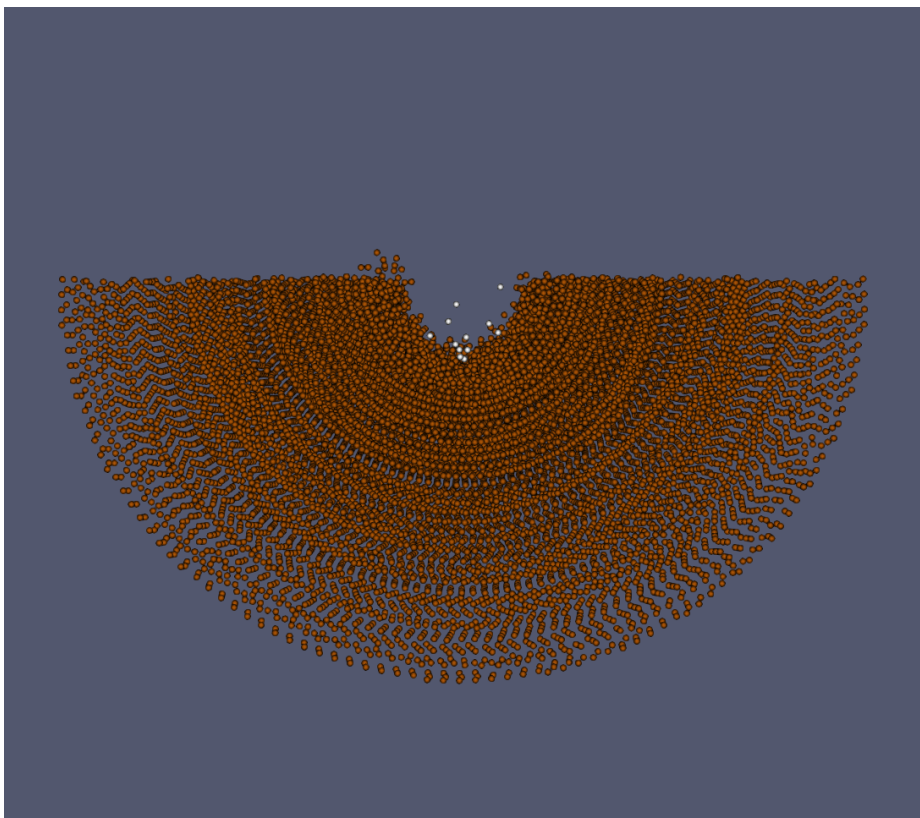


Figure 6: High porosity (50%), high strength ($Y=1\text{ MPa}$)

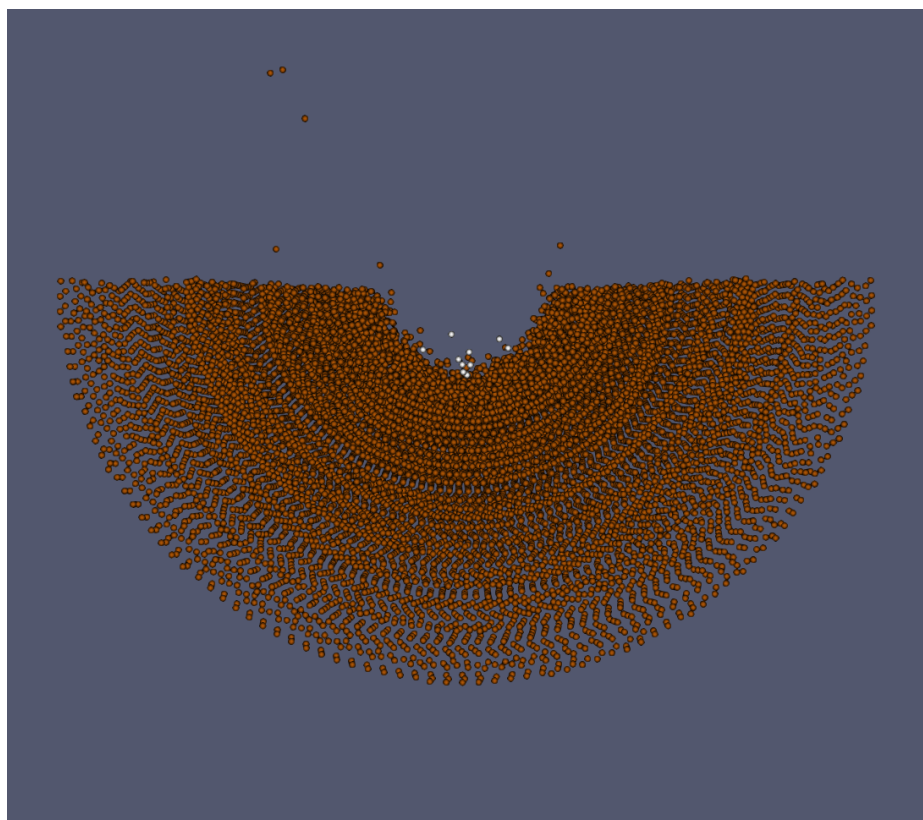


Figure 7: High porosity (50%), low strength ($Y=1\text{kPa}$)

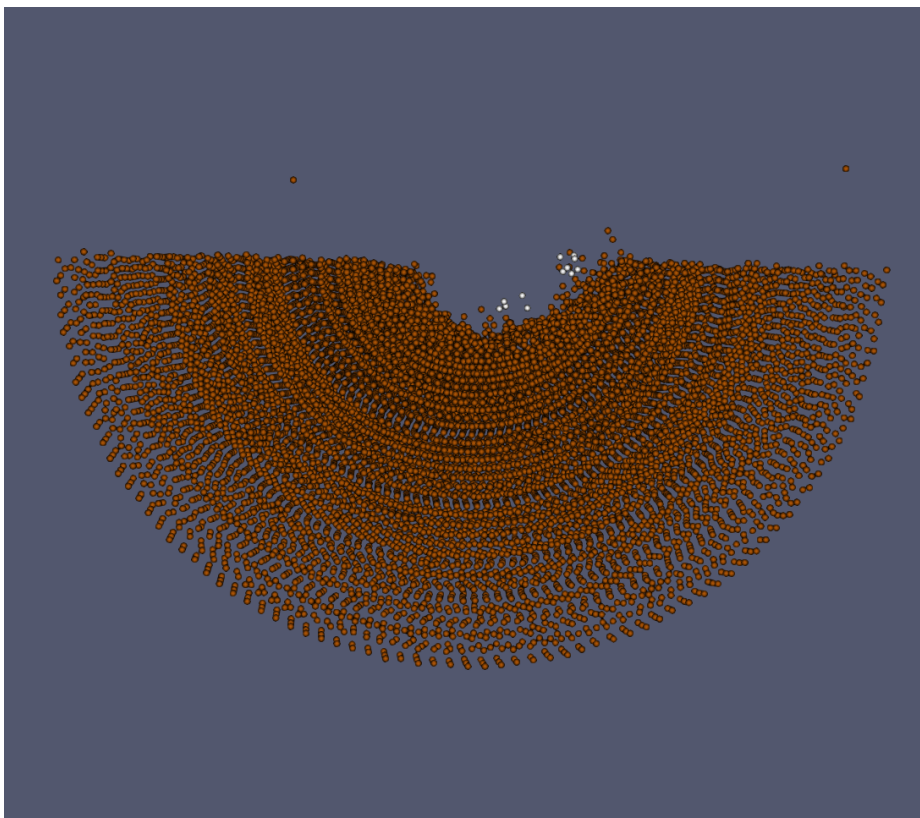


Figure 8: High porosity (50%), low strength ($Y=1\text{kPa}$), 45 degree angle

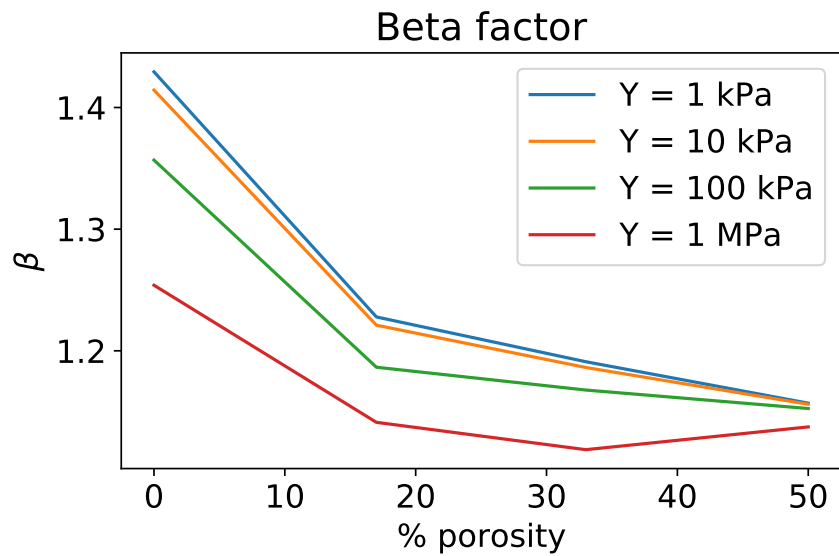


Figure 9: beta factor

5 Discussion

- beta factor on the lower end - upper limit beta $\downarrow 2$ because of momentum conservation??
- tensorial correction not implemented because of timestep getting to small

References

- [1] J. H. Tillotson. "Metallic Equations of State For Hypervelocity Impact". In: (July 1962), p. 3216.
- [2] R. A. Gingold and J. J. Monaghan. "Smoothed particle hydrodynamics: theory and application to non-spherical stars". In: *Monthly Notices of the Royal Astronomical Society* 181.3 (Dec. 1977), pp. 375–389. ISSN: 0035-8711. DOI: 10.1093/mnras/181.3.375. eprint: <https://academic.oup.com/mnras/article-pdf/181/3/375/3104055/mnras181-0375.pdf>. URL: <https://doi.org/10.1093/mnras/181.3.375>.
- [3] Martin Jutzi, Willy Benz, and Patrick Michel. "Numerical simulations of impacts involving porous bodies". In: *Icarus* 198.1 (Nov. 2008), pp. 242–255. ISSN: 0019-1035. DOI: 10.1016/j.icarus.2008.06.013. URL: <http://dx.doi.org/10.1016/j.icarus.2008.06.013>.
- [4] C. Schaefer et al. "A smooth particle hydrodynamics code to model collisions between solid, self-gravitating objects". In: *Astronomy and Astrophysics* 590 (Apr. 2016), A19. ISSN: 1432-0746. DOI: 10.1051/0004-6361/201528060. URL: <http://dx.doi.org/10.1051/0004-6361/201528060>.
- [5] A.M. Stickle et al. "Modeling impact outcomes for the Double Asteroid Redirection Test (DART) mission". In: *Procedia Engineering* 204 (2017). 14th Hypervelocity Impact Symposium 2017, HVIS2017, 24-28 April 2017, Canterbury, Kent, UK, pp. 116–123. ISSN: 1877-7058. DOI: <https://doi.org/10.1016/j.proeng.2017.09.763>. URL: <http://www.sciencedirect.com/science/article/pii/S1877705817343217>.
- [6] Sabina Raducan et al. "The role of asteroid strength, porosity and internal friction in impact momentum transfer". In: *Icarus* 329 (Apr. 2019), pp. 282–295. DOI: 10.1016/j.icarus.2019.03.040.
- [7] Wikimedia Commons. *File:SmallAsteroidImpacts-Frequency-Bolide-20141114.jpg* — *Wikimedia Commons, the free media repository*. [Online; accessed 20-September-2020]. 2020. URL: <https://commons.wikimedia.org/w/index.php?title=File:SmallAsteroidImpacts-Frequency-Bolide-20141114.jpg&oldid=447357435>.
- [8] Wikimedia Commons. *File:SPHInterpolationColorsVerbose.svg* — *Wikimedia Commons, the free media repository*. [Online; accessed 20-September-2020]. 2020. URL: <https://commons.wikimedia.org/w/index.php?title=File:SPHInterpolationColorsVerbose.svg&oldid=446219914>.